Title

The effect of humic acid on the aggregation of titanium dioxide nanoparticles under different pH and ionic strengths

Journal

The Science of The Total Environment, 487(1)

ISSN

0048-9697

Authors

Zhu, Miao
Wang, Hongtao
Keller, Arturo A
et al.

Publication Date

2014-07-01

DOI

10.1016/j.scitotenv.2014.04.036

Peer reviewed

Science of the Total Environment 487 (2014) 375–380

Contents lists available at ScienceDirect

Science of the Total Environment

journal homepage: www.elsevier.com/locate/scitotenv

The effect of humic acid on the aggregation of titanium dioxide nanoparticles under different pH and ionic strengths

Miao Zhu [a,1], Hongtao Wang [a,*], Arturo A. Keller [b,1], Tao Wang [a,1], Fengting Li [a,1]

[a] Key Laboratory of Yangtze River Water Environment, Ministry of Education, State Key Laboratory of Pollution Control and Resource Reuse, College of Environmental Science and Engineering, Tongji University, Shanghai 200092, China
[b] Bren School of Environmental Science and Management, University of California, Santa Barbara, CA 93106, United States

HIGHLIGHTS

- Charge neutralization was observed when pH = 4 and ionic strength is very low.
- Steric hindrance only occurs when ionic strength is lower than CCC.
- Humic acid plays a bridging effect when ionic strength is higher than CCC.

GRAPHICAL ABSTRACT

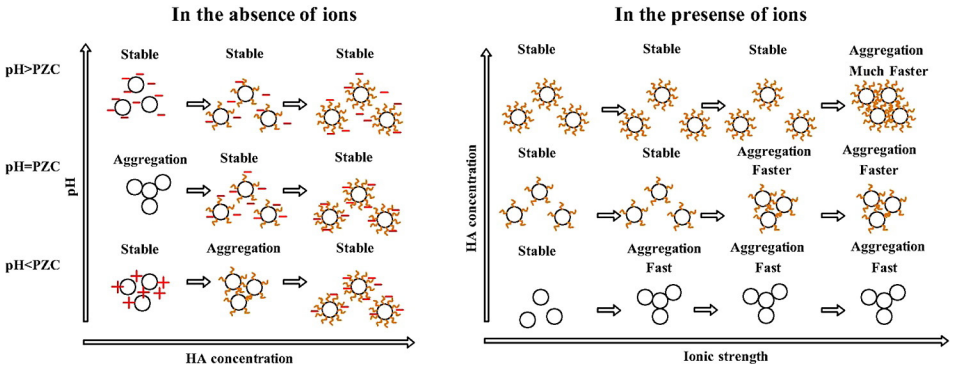

ARTICLE INFO

Article history:
Received 19 November 2013
Received in revised form 7 April 2014
Accepted 8 April 2014
Available online xxxx

Editor: Kevin V. Thomas

Keywords:
Humic acid
Titanium dioxide
Nanoparticles
Critical coagulation concentration
Aggregation
Ionic strength

ABSTRACT

With the increasingly widespread use of titanium dioxide nanoparticles (TiO_2 NPs), the particles' environmental impacts have attracted concern, making it necessary to understand the fate and transport of TiO_2 NPs in aqueous media. In this study, we investigated TiO_2 NP aggregation caused by the effects of humic acid (HA), ionic strength (IS) and different pH using dynamic light scattering (DLS) to monitor the size distribution of the TiO_2 NPs continuously. It was determined that HA can influence the stability of TiO_2 NPs through charge neutralization, steric hindrance and bridging effects. In the absence of IS, aggregation was promoted by adding HA only when the pH (pH = 4) is less than the point of zero charge for the TiO_2 NPs ($pH_{PZC} \approx 6$) because HA reduces the zeta potential of the TiO_2 NPs via charge neutralization. At pH = 4 and when the concentration of HA is 94.5 μg/L, the zeta potential of TiO_2 NPs is close to zero, and they reach an aggregation maximum. A higher concentration of HA results in more negatively charged TiO_2 NP surfaces, which hinder their aggregation. When the pH is 5.8, HA enhances the negative zeta potential of the TiO_2 NPs and increases their stability via electrostatic repulsion and steric hindrance. When the pH (pH = 8) is greater than pH_{pzc}, the zeta potential of the TiO_2 NPs is high (~40 mV), and it barely changes with increasing HA concentration. Thus, the TiO_2 NPs are notably stable, and their size does not grow at pH 8. The increase in the critical coagulation concentration (CCC) of TiO_2 NPs indicated that there is steric hindrance after the addition of HA. HA can enhance the coagulation of TiO_2 NPs, primarily due to bridging effect. These findings are useful in understanding the size change of TiO_2 NPs, as well as the removal of TiO_2 NPs and HA from aqueous media.

* Corresponding author. Tel.: +86 21 65980567; fax: +86 21 65985059.
E-mail address: hongtao@tongji.edu.cn (H. Wang).
[1] Tel.: +86 21 65980567; fax: +86 21 65985059.

http://dx.doi.org/10.1016/j.scitotenv.2014.04.036
0048-9697/

1. Introduction

The application of nanotechnology in consumer and industrial products has increased exponentially over the past several years. Nanomaterials are widely used in herbicides, cosmetics, printers, electronics, groundwater remediation, waste water treatment, and many other applications (Keller et al., 2013; Theron et al., 2008). The toxicity of nanomaterials is determined by their size, shape, chemical structure and surface properties. It is imperative to evaluate the potential risks that these novel materials pose to the environment and human health, and the first step is to assess their mobility in the environment (Wiesner et al., 2006).

During the recent years, the potential risks of nanoparticles have raised concerns. The cytotoxicity of TiO_2 NPs has been discussed (Jin et al., 2008). It has been reported that TiO_2 NPs can cause respiratory toxicity and disturbances in metabolism (Federici et al., 2007). A single intratracheal injection of 0.1 mg nanoTiO_2 can induce severe pulmonary inflammation and emphysema (Chen et al., 2006). TiO_2 NPs can induce clastogenicity, genotoxicity, oxidative DNA damage, and inflammation (Trouiller et al., 2009). In addition, under low intensity UVR, ROS in seawater increases with increasing nano-TiO_2 concentration, which leads to increased overall oxidative stress in seawater, and causes decreased resiliency of marine ecosystems (Miller et al., 2012). Nano-TiO_2 had positive effects on root elongation in some species (Song et al., 2013). TiO_2 NPs have cytotoxic, genotoxic and hemolytic effects on human erythrocyte and lymphocyte cells in vitro and can induce a significant reduction in mitochondrial dehydrogenase activity in human lymphocyte cells (Ghosh et al., 2013). Nanoparticles can be transported in the human body, deposited in organs, transferred across cell membranes and accumulated in mitochondria, causing damage to humans (Colvin, 2003).

To some extent, the size range of nanoparticles in natural water determines their stability, toxicity, transport and ultimate fate (Zhang et al., 2008, 2012). As reported, the size of nanoparticles is related to solution chemistry, typically including natural organic matter (NOM), ions and pH, and it was also found that three nanoparticles (TiO_2, ZnO, CeO_2) can aggregate easily when the IS is high and the total organic carbon (TOC) is low; conversely, their stability is high when the TOC is high for a wide range of IS, but not at very high IS (Keller et al., 2010). NOM in aquatic systems has a significant effect on the transport and transformation of the nanoparticles, and the nanoparticles' adsorption capacity toward hydrophobic organic compounds (HOCs) will change their stability and toxicity (Adegboyega et al., 2013; Baalousha et al., 2013; Louie et al., 2013; Wirth et al., 2012; Yang et al., 2009; Zhang et al., 2013). NOM is also commonly present in ground water and surface water, although at different concentrations (Wang et al., 2010, 2011). These macromolecules can be adsorbed onto the surfaces of the nanoparticles, enhancing their stability and mobility in flowing waters (Chappell et al., 2009; Hyung et al., 2007). The adsorption capacity of the nanoparticles is related to the pH, and NOM is absorbed by the nanoparticles' surface via electrostatic adsorption and ligand exchange (mainly hydroxyl and carboxyl groups). The adsorption of NOM reduces the surface zeta potential and changes the electrostatic repulsion, which affects the nanoparticle stability (Yang et al., 2009).

Humic substances (HS) represent an active and important fraction of natural organic matter (NOM), and they play important roles in the fate and transport of pollutants (Aiken, 1985; Buffle et al., 1998; Zheng et al., 2008). HS can be categorized into three groups: fulvic acids (FAs), which are the major component and the smallest structures of HS, and are soluble at any pH; HA, which represents bigger structures that are insoluble at pH <2; and humin, which is insoluble at any pH (Jones and Bryan, 1998; Piccolo, 2001). The role of HA in nanoparticle transport is of particular interest. The fate of fullerenes (nC_{60}) and their toxic implications in natural freshwaters are affected by humic acid (Meng et al., 2013; Pakarinen et al., 2013), and humic acid is more effective than fulvic acid at stabilizing nC_{60} nanoparticles (Zhang et al., 2013). Humic acid affects the adsorption of other pollutants on the surface of multiwalled carbon nanotubes (MWCNTs) (Hou et al., 2013). Humic acid also reduces the removal of TiO_2 NPs via coagulation (Wang et al., 2013).

TiO_2 NPs are some of the most widely used nanoparticles. Most TiO_2 NPs are used for coatings, paints, and pigments as well as cosmetics (Keller et al., 2013). In 2010, over 34,000 t of TiO_2 NPs were used in coatings, paints, and pigments, and TiO_2 is by far the most significant engineered nanoparticle materials in terms of exposure, based on the estimated releases and use in the dominant applications (Keller and Lazareva, 2013). At the nanoscale, the refractive index of TiO_2 NPs is even higher; therefore, it is also used in sunscreens and cosmetics as well as paints, varnishes, and coatings (Hendren et al., 2011). The adsorption of HA increased TiO_2 NP stability in suspension, and TiO_2 NPs were more toxic in the presence of HA (Yang et al., 2013). It was demonstrated that the aggregation of TiO_2 NPs is dependent on the presence and copresence of NOM (0.2–41.1 mg/L DOC), the pH of the solution, as well as other properties, such as the IS of the solution and the presence of relevant monovalent and divalent ions (Ottofuelling et al., 2011). Zhang et al. tested the stability of TiO_2 at various DOC concentrations (1–10 mg/L NOM, equivalent to 0.406–4.06 mg/L DOC) and observed the stability in the presence of 0.4 mg/L DOC (Zhang et al., 2009). However, it is not clear if a very low concentration of NOM (e.g., <0.2 mg/L DOC) has the same effect on the stability of TiO_2 NPs; a low concentration of DOC is possible in some industrial wastewater.

The goal of this study was to study the effect of HA on the aggregation or stabilization of TiO_2 NPs under different pH and ISs. We chose three typical pH: pH = 4 (pH < pH_{pzc}); pH = 5.8 (pH = pH_{pzc}); and pH = 8 (pH > pH_{pzc}). Because TiO_2 NPs are very stable at pH = 8, we also measured the critical coagulation concentration (CCC) to further investigate the role of HA in the stabilization of TiO_2 NPs at high pH. Finally, to compare the different CCCs at pH = 4 and pH = 8, we studied the aggregation and sedimentation performances under high IS (>CCC).

2. Materials and methods

2.1. Titanium dioxide nanoparticles

NanoTiO_2 (rutile) was purchased from Sigma-Aldrich Trading Co., Ltd. (Shanghai, China). As reported by the manufacturer, these nanoparticles have a diameter × length of 10 nm × 40 nm; specific surface area = 130–190 m^2/g; purity = 99.5%; and may contain up to 5 wt.% silicon dioxide as a surface coating. In our recent publication (Qi et al., 2013), we used scanning electron microscopy (SEM) images and transmission electron microscopy (TEM) images to characterize the size and shape of the TiO_2 NPs. The primary size of the TiO_2 NPs is within the reported range. The pH_{PZC} of the TiO_2 NPs was measured using a Malvern Zetasizer (Nano ZS 90, UK). It was found that the pH_{PZC} of the TiO_2 NPs is ~6 (Fig. S1). A 1-g/L TiO_2 NP stock suspension was prepared by weighing an appropriate amount of dry powder, mixing it with deionized water, and sonicating the suspension for 20 min (Qi et al., 2013). The TiO_2 NP suspension was added into a small glass bottle and dispersed using a Nishang Ultrasonics SY-180 (power, 180 W, nominal frequency, 40 kHz, Shanghai, China). In order to control water temperature inside the sonicator, circulating cooling water was used, which maintained the water temperature at 19 °C. Each ultrasound time was 60 s, and interval time was 5 s. Our previous experiments indicated that this method is able to disperse the TiO_2 NPs to meet the requirement for the following tests. A fresh stock suspension was prepared daily.

2.2. Humic acid

The humic acid was purchased from Sigma-Aldrich (Shanghai) Trading Co., Ltd. An HA stock solution was prepared by dissolving a certain amount of HA powder into deionized water, adjusting the pH to 11 by adding 0.1 M NaOH, and then stirring the solution at 600 rpm

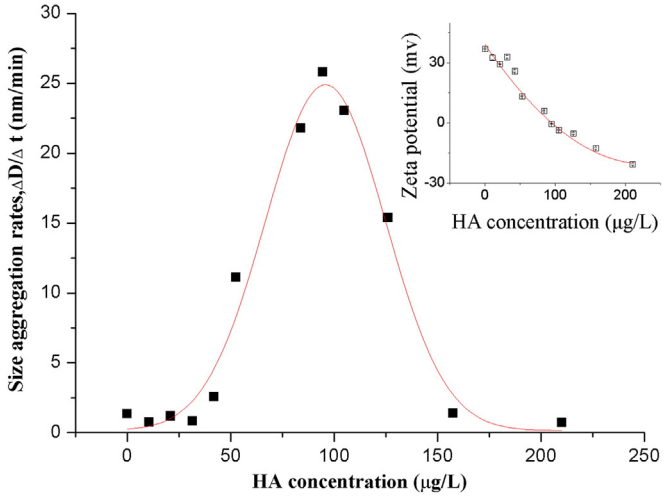

Fig. 1. The aggregation of TiO_2 NPs as a function of HA concentration when pH = 4 (pH < pH_{PZC}). (Sodium acetate–acetic acid buffer; TiO_2 NP concentration is 20 mg/L).

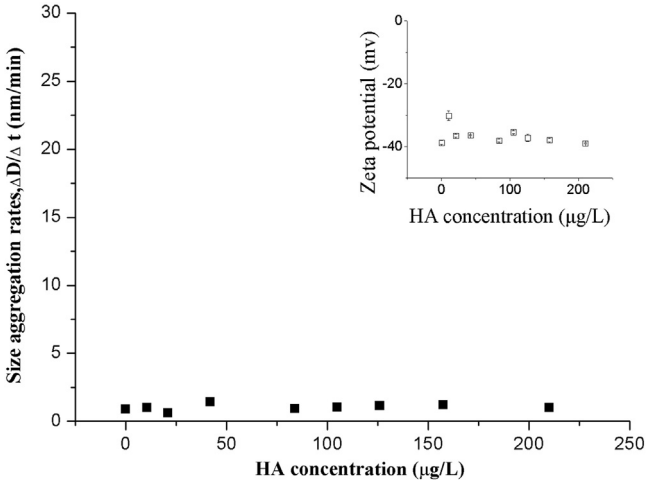

Fig. 3. The aggregation of TiO_2 NPs as a function of the HA concentration when pH = 8 (pH > pH_{PZC}). (Borate buffer; TiO_2 NP concentration = 20 mg/L).

for 24 h to improve the solution stability. A 0.25-μm filter membrane was used to remove the insoluble matter. The stock solution was stored under 5 °C. The total organic carbon (TOC) of the HA stock solution was measured using a Shimadzu TOC-V, and the stock solution was diluted to 10.5 mg/L TOC.

2.3. Buffer solution preparation

In this study, two types of buffer solutions were used to control the pH: sodium acetate–acetic acid buffer and boric acid–borax buffer. The sodium acetate–acetic acid buffer can control the pH between ~4 and 5.8, and the boric acid–borax buffer can control pH of ~8. All of the buffers were diluted 200 times in the test.

2.4. Aggregation rates and coagulation kinetics

The aggregation rates and coagulation kinetics were measured by collecting time-resolved hydrodynamic size data of the particle suspension using dynamic light scattering (DLS) (Zetasizer nano, Malvern, UK). All of the size data were Z-averaged (mean size), which were calculated using cumulant analysis. The cumulant analysis only gives two values, a mean value for the size, and a width parameter known as the Polydispersity Index (PDI). It is important to note that this mean size (often given the symbol Z or z-average) is an intensity mean. It is not a mass or number mean because it is calculated from the signal intensity. The DLS measurements were started immediately after mixing. Each measurement lasted for 30 s. The instrument employed a 633-nm laser with a detection angle of 90°. For aggregation rate measurements, the concentration of the TiO_2 NPs was 20 mg/L, and the concentration range of HA was 0–210 μg/L. Each reaction was measured continuously for 20 min. The aggregation rates are expressed as the slope ΔD/Δt (nm/min), where ΔD means the increase in the TiO_2 NP diameters (nm) and Δt denotes the time range (min). For the coagulation kinetics measurements, the concentration of the TiO_2 NPs was 10 mg/L, and the concentrations of HA were 1, 5, and 10 mg/L. NaCl was used to provide the IS. The concentration range of NaCl was 0 to 4.5 mol/L. Data were collected for either 1 h or until the hydrodynamic diameter doubled, depending on whichever criteria were met first (Zhou et al., 2012). The suspension stability was analyzed by examining the variation of the attachment efficiency α with IS. α is defined as the ratio of the coagulation rate in the presence of an energy barrier to that in the absence of an energy barrier (Elimelech et al., 1995):

$$\alpha = \frac{k}{k_{fast}} = \frac{\left(\frac{d_{r_H}}{d_t}\right)_{t\to 0}}{\left(\frac{d_{r_H}}{d_t}\right)_{t\to 0,\mathrm{fast}}}.$$

In this equation, r_H is the hydrodynamic radius; $(d_{rH}/d_t)_{t\to 0,\mathrm{fast}}$ is calculated as the average of the highest, relatively constant rates observed experimentally for a given set of conditions. Therefore, the relationship between α and IS identifies the critical coagulation concentration (CCC), which marks the IS at which α reaches the constant value of unity (Zhou et al., 2012).

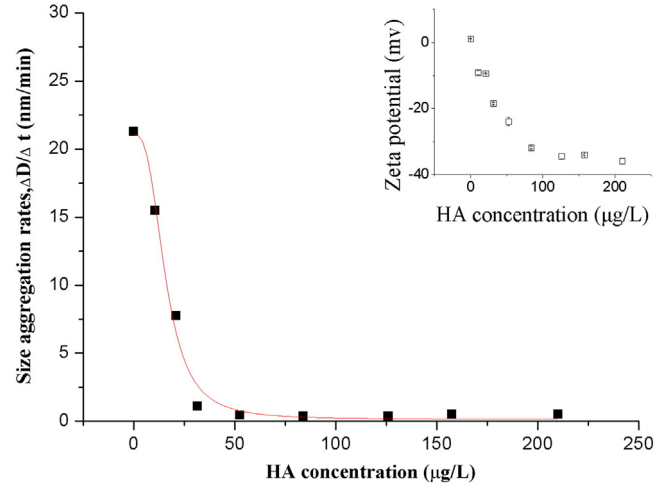

Fig. 2. The aggregation of TiO_2 NPs as a function of the HA concentration when pH = 6 (pH = pH_{PZC}). (Sodium acetate–acetic acid buffer; TiO_2 NP concentration is 20 mg/L).

Table 1
CCC of TiO_2 NPs at pH = 4 and 8 under different HA concentrations.

HA concentration (TOC, mg/L)	CCC (NaCl, mmol/L)	
	pH = 4	pH = 8
0	75	50
1	350	800
5	600	>4500
10	1200	>4500

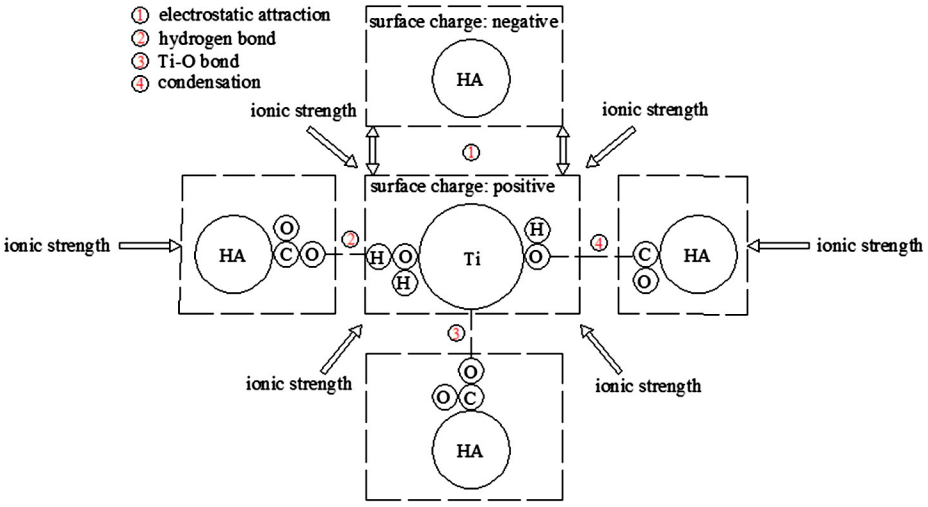

Fig. 4. The effect of pH on the HA-NP aggregation pathways in NaCl electrolyte (pH = 4).

2.5. Sedimentation measurements

The sedimentation rate was determined by measuring the turbidity of the supernatant (HACH 2100P turbidity meter). The HA concentration varied from 0 to 10 mg/L. A sodium acetate–acetic acid buffer was used to control the pH at 4. The concentration of the TiO_2 NPs was 10 mg/L. Sodium chloride was used to provide the IS, and its concentration was 3 mol/L. The maximum aggregation and sedimentation rates with different HA concentrations can be reached under these conditions. The sedimentation measurements lasted for 30 h.

3. Results and discussion

3.1. TiO_2-NP stability as a function of HA concentration

At pH = 4 ($pH < pH_{pzc}$) and in the absence of HA, the zeta potential of the TiO_2 NPs is 37 mV (Fig. S1). With the addition of 210 μg/L HA, the zeta potential decreases to −20.6 mV (Fig. 1 inset). Fig. S2 shows that HA carries negative charge when pH ranges from 4 to 8. The charge of the hydrophobic fraction of NOM is associated mainly with the carboxylic and phenolic groups (Duffy, 2010; Edwards et al., 1996). The former have pK_a values in the range between 2.5 and 5, while the phenolic hydrogens have pK_a values around 9 or 10 (Duffy, 2010). As a result, humic acid is negatively charged due to ionization of carboxylic groups in the pH range of natural waters. At [HA] = 94.5 μg/L, the zeta potential is approximately 0 mV, and the TiO_2 NPs reach the maximum aggregation rate (Fig. 1). When the addition of HA is less than 94.5 μg/L, the aggregation rate increases with increasing HA concentration, which is due to the charge neutralization of the TiO_2 NPs by the adsorbed HA and confirmed by the decreasing zeta potential of the TiO_2 NPs. However, when the HA concentration is greater than 94.5 μg/L, the aggregation rate decreases with higher HA concentrations because the surface charge is reversed. When the zeta potential is greater than +20 mV or less than −20 mV, the TiO_2 NPs are very stable and their aggregation rate is close to zero. In summary, when pH is $<pH_{pzc}$, the effect of HA on TiO_2 NP stability can be divided into two phases: (a) HA neutralizes and reduces the surface charge of the TiO_2 NPs and promotes the aggregation of TiO_2 NPs, (b) excessive addition of HA reverses the surface charge and makes the TiO_2 NPs more stable.

The aggregation of TiO_2 NPs at pH = 5.8 is shown in Fig. 2. Sodium acetate–acetic acid buffer was used to control the pH. Because 5.8 is very close to the pH_{pzc}, it can be observed that the initial zeta potential is close to zero and the aggregation rate is very fast when the HA concentration is 0 μg/L. No obvious aggregation is observed when the HA concentration is greater than 31.5 μg/L. At this HA concentration, the zeta potential of the TiO_2 NPs is approximately −20 mV, which stabilizes the TiO_2 NPs via electrostatic repulsion. Fig. 2 also shows

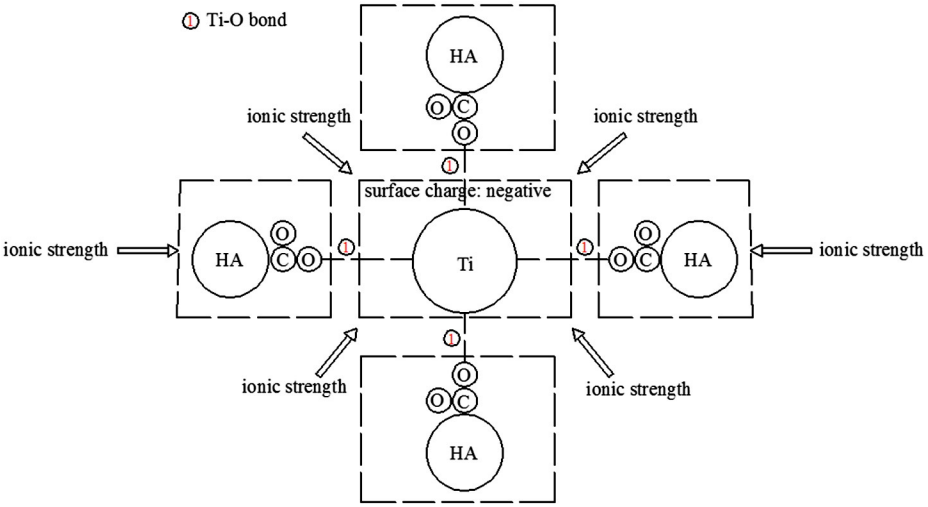

Fig. 5. The effect of pH on the HA-NP aggregation pathways in NaCl electrolyte (pH = 8).

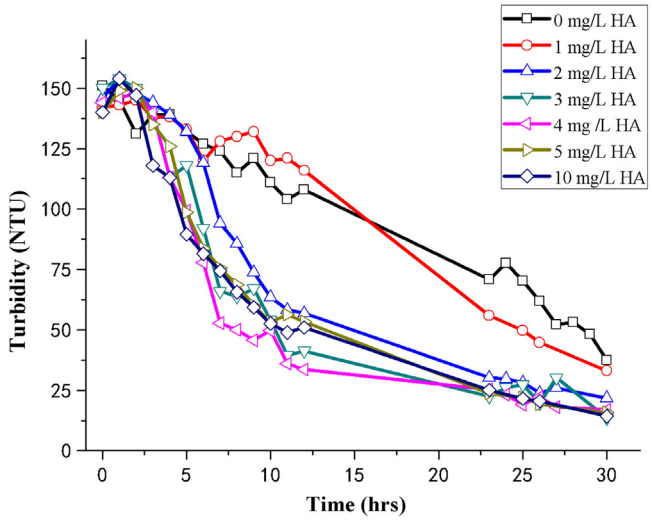

Fig. 6. The turbidity of supernatant after 30 h when pH = 4 and NaCl concentration = 3 mol/L.

that when zeta potential is within 0 mV to −10 mV, the aggregation rate is relatively fast, and when the zeta potential is lower than −20 mV, the aggregation rate is close to zero and the suspension is very stable. When the HA concentration is greater than 84 μg/L, the zeta potential of TiO_2 NPs barely changes with the addition of HA. In this situation (pH = pH_{pzc} = 5.8), the addition of HA makes the suspension more stable via electrostatic repulsion.

At pH = 8 (pH > pH_{pzc}) and in the absence of HA, the zeta potential is −38.7 mV, and the aggregation rate is close to zero (Fig. 3). The zeta potential is barely sensitive to the addition of HA at this pH (Fig. 3 inset); the suspension is very stable regardless of the presence of HA in the system.

3.2. Coagulation kinetics measurements

The CCC of TiO_2 NPs in the presence and absence of HA was measured at pH = 4 and pH = 8. The concentrations of HA were 1, 5, and 10 mg/L, and the TiO_2 NP concentration was 10 mg/L. Figs. S3 and S4 show that the aggregation speed increased with increasing ionic strength. This phenomenon indicates that increasing the ionic strength compresses the double layer, causing a decrease in its thickness, which results in a decreased zeta potential, and therefore, the energy barrier was reduced and the particles rapidly aggregate (Chen and Elimelech, 2007; Overbeek and Kruyt, 1952; Thio et al., 2011; Verwey and Overbeek, 2001). As Fig. S3 and Table 1 indicate, the TiO_2 NP suspension was more stable at pH 4 (CCC ≈ 75 mmol/L) than at pH 8 (CCC ≈ 50 mmol/L). However, in the presence of HA, it is shown in Fig. S4 and Table 1 that the TiO_2-NP suspension is more stable at pH 8 than at pH 4. At pH 4, the CCC of the TiO_2 NPs is 600 mmol/L when the HA concentration is 5 mg/L, and the CCC is 1200 mmol/L when the HA concentration is 10 mg/L. At pH = 8, the CCC is greater than 4500 mmol/L at both HA concentrations. With the addition of HA, the TiO_2 NP suspension becomes more stable. Fig. 4 indicates that the addition of HA barely changes the zeta potential or the aggregation rate at pH 8. Comparing Figs. S3, S4, S5 and Table 1, it can be observed that HA still plays an important role in stabilizing the TiO_2 NPs, although it barely changes the surface charge at pH = 8. The steric hindrance provided by the adsorbed HA limits the interactions between the TiO_2 NPs and NaCl, so that the CCC of TiO_2 NPs increases in the presence of HA.

NOM is negatively charged in natural waters. It can be associated with TiO_2 NPs through electrostatic attraction. Theoretical and experimental studies on the adsorption of various organic compounds onto TiO_2 indicate that the carboxyl and phenolic functional groups in NOM can bind to Ti or O atoms on the TiO_2 surface (Langel and Menken, 2003; Persson and Lunell, 2000; Roddick-Lanzilotta and McQuillan, 2000).

At pH = 4, as shown in Fig. 4, there are four possible ways for the TiO_2 NPs to adsorb HA: electrostatic attraction, hydrogen bonding, Ti–O bonding and condensation (Liu et al., 2008). The charge of HA is negative, and the surface charge of the TiO_2 NPs is positive, so adsorption occurs through electrostatic attraction at pH < pH_{PZC}. As shown in Fig. 4, the HA adsorbed by the TiO_2 NPs has steric hindrance that limits the TiO_2 NPs from getting close to the secondary or primary minima. Through this mechanism, the CCC increases from 75 mmol/L to 350 mmol/L with the addition of 1 mg/L HA at pH 4 (Figs. S3, S4 and Table 1). However, at pH 8, as shown in Fig. 5, there is only one mechanism (Ti–O bonding) for the TiO_2 NPs to adsorb to the HA. Under these conditions, both the surface charge on the TiO_2 NPs and the charge of HA are negative, so electrostatic repulsion limits the adsorption of HA to the TiO_2 NPs. Based on a comparison of Figs. S3 and S4, it can be observed that the CCC increases from 50 mmol/L to 800 mmol/L at pH 8 when 1 mg/L of HA was added, which can be explained as follows: (a) HA has steric hindrance that hinders the TiO_2 NP interaction with the ions; and (b) these chemical bonds reduce the reactivity of the hydroxide radicals on the surface of the TiO_2 NPs.

3.3. Sedimentation measurements

As shown in Fig. S4 and Table 1, the CCCs of TiO_2 NPs at pH = 4 are 75 mmol/L, 350 mmol/L, 600 mmol/L and 1200 mmol/L when the HA concentrations were 0, 1, 5, and 10 mg/L, respectively, and 3 mol/L NaCl was added to the solution to ensure that the IS is higher than the CCC. Acetate buffer (pH = 4) was used to control the pH. Fig. S5 indicates that, upon addition of HA, the aggregation rates increase, which can be observed from Fig. 6 (i.e., the TiO_2 NPs have a faster sedimentation rate in the presence of HA than the control, which lacks HA). This result can be explained by the bridging effect of HA. In the presence of HA at pH 4, the surface of the TiO_2 NPs will adsorb HA through four mechanisms as previously mentioned. As macromolecules with long chains, HA can tangle the TiO_2 NPs through a "bridging effect" (Tan et al., 2009). Fig. S7 indicates that the flocs became bigger as more HA is added. In addition, the color of the flocs became darker as HA was added. Additionally, Fig. S8 shows that NOM is absorbed by the TiO_2 NPs, which became a sediment, so only a small amount of HA remained in the supernatant, proving the existence of a bridging effect and the entanglement effect of HA.

4. Conclusions

Our results indicated that HA plays different roles under different pH and IS conditions. When the IS is very low, the aggregation of the TiO_2 NPs is promoted by the adsorption of HA only when the TiO_2 NP surface is positively charged. When the pH is below the pH_{pzc}, the addition of HA reduces the zeta potential of the TiO_2 NPs and reverses the surface charge of the TiO_2 NPs. When the pH is close to the pH_{pzc}, a low concentration of HA (31.5 μg/L) can stabilize 20 mg/L of TiO_2 NPs by altering their surface charge to be more negative. When the pH is greater than the pH_{pzc}, the presence of HA does not change the zeta potential of the TiO_2 NPs, but it stabilizes the TiO_2 NPs via steric hindrance and ligand exchange. These findings indicate that very low concentrations (<0.21 mg/L) of NOM can stabilize or destabilize TiO_2 NPs (20 mg/L) at different pH. When the IS is higher than the CCC, the HA has a bridging effect, which promotes the aggregation and sedimentation rates of the TiO_2 NPs. In conclusion, HA has different effects on the aggregation and stabilization of TiO_2 NPs, and these effects are influenced by the pH and IS values.

Conflict of interest statement

We declare that we have no financial and personal relationships with other people or organizations that can inappropriately influence our work, there is no professional or other personal interest of any nature or kind in any product, service or company that could be construed as influencing the position presented in, or the review of, the manuscript entitled.

Acknowledgments

This work was supported in part by the National Natural Science Foundation of China Fund (No. 51108328). The research was also partially supported by 111 Project and the Fundamental Research Funds for the Central Universities (0400219184) and State Key Laboratory of Pollution Control and Resource Reuse Foundation (No. PCRRY11011).

Appendix A. Supplementary data

Supplementary data to this article can be found online at http://dx.doi.org/10.1016/j.scitotenv.2014.04.036.

References

Adegboyega NF, Sharma VK, Siskova K, Zboril R, Sohn M, Schultz BJ, et al. Interactions of aqueous Ag^+ with fulvic acids: mechanisms of silver nanoparticle formation and investigation of stability. Environ Sci Technol 2013;47:757–64.
Aiken G. Humic substances in soil, sediment, and water: geochemistry, isolation, and characterization. New York: Wiley; 1985.
Baalousha M, Nur Y, Romer I, Tejamaya M, Lead JR. Effect of monovalent and divalent cations, anions and fulvic acid on aggregation of citrate-coated silver nanoparticles. Sci Total Environ 2013;454:119–31.
Buffle J, Wilkinson KJ, Stoll S, Filella M, Zhang JW. A generalized description of aquatic colloidal interactions: the three-colloidal component approach. Environ Sci Technol 1998;32:2887–99.
Chappell MA, George AJ, Dontsova KM, Porter BE, Price CL, Zhou PH, et al. Surfactive stabilization of multi-walled carbon nanotube dispersions with dissolved humic substances. Environ Pollut 2009;157:1081–7.
Chen HW, Su SF, Chien CT, Lin WH, Yu SL, Chou CC, et al. Titanium dioxide nanoparticles induce emphysema-like lung injury in mice. Faseb J 2006;20:2393.
Chen KL, Elimelech M. Influence of humic acid on the aggregation kinetics of fullerene (C_{60}) nanoparticles in monovalent and divalent electrolyte solutions. J Colloid Interface Sci 2007;309:126–34.
Colvin VL. The potential environmental impact of engineered nanomaterials. Nat Biotechnol 2003;21:1166–70.
Duffy SJ. Environmental chemistry: a global perspective. Oxford University Press; 2010.
Edwards M, Benjamin MM, Ryan JN. Role of organic acidity in sorption of natural organic matter (NOM) to oxide surfaces. Colloids Surf A Physicochem Eng Asp 1996;107:297–307.
Elimelech M, GJ, Jia X, Williams R. Particle deposition and aggregation: measurement. New York: Elsevier; 1995.
Federici G, Shaw BJ, Handy RD. Toxicity of titanium dioxide nanoparticles to rainbow trout (oncorhynchus mykiss): gill injury, oxidative stress, and other physiological effects. Aquat Toxicol 2007;84:415–30.
Ghosh M, Chakraborty A, Mukherjee A. Cytotoxic, genotoxic and the hemolytic effect of titanium dioxide (TiO2) nanoparticles on human erythrocyte and lymphocyte cells in vitro. J Appl Toxicol 2013;33:1097–110.
Hendren CO, Mesnard X, Droge J, Wiesner MR. Estimating production data for five engineered nanomaterials as a basis for exposure assessment. Environ Sci Technol 2011;45:2562–9.
Hou L, Zhu DQ, Wang XM, Wang LL, Zhang CD, Chen W. Adsorption of phenanthrene, 2-naphthol, and 1-naphthylamine to colloidal oxidized multiwalled carbon nanotubes: effects of humic acid and surfactant modification. Environ Toxicol Chem 2013;32:493–500.
Hyung H, Fortner JD, Hughes JB, Kim JH. Natural organic matter stabilizes carbon nanotubes in the aqueous phase. Environ Sci Technol 2007;41:179–84.
Jin CY, Zhu BS, Wang XF, Lu QH. Cytotoxicity of titanium dioxide nanoparticles in mouse fibroblast cells. Chem Res Toxicol 2008;21:1871–7.
Jones MN, Bryan ND. Colloidal properties of humic substances. Adv Colloid Interface Sci 1998;78:1–48.
Keller AA, Lazareva A. Predicted releases of engineered nanomaterials: from global to regional to local. Environ Sci Technol Lett 2013.
Keller AA, McFerran S, Lazareva A, Suh S. Global life cycle releases of engineered nanomaterials. J Nanoparticle Res 2013;15:1–17.
Keller AA, Wang HT, Zhou DX, Lenihan HS, Cherr G, Cardinale BJ, et al. Stability and aggregation of metal oxide nanoparticles in natural aqueous matrices. Environ Sci Technol 2010;44:1962–7.
Langel W, Menken L. Simulation of the interface between titanium oxide and amino acids in solution by first principles MD. Surf Sci 2003;538:1–9.
Liu GJ, Zhang XR, Talley JW, Neal CR, Wang HY. Effect of NOM on arsenic adsorption by TiO2 in simulated As(III)-contaminated raw waters. Water Res 2008;42:2309–19.
Louie SM, Tilton RD, Lowry GV. Effects of molecular weight distribution and chemical properties of natural organic matter on gold nanoparticle aggregation. Environ Sci Technol 2013;47:4245–54.
Meng ZY, Hashmi SM, Elimelech M. Aggregation rate and fractal dimension of fullerene nanoparticles via simultaneous multiangle static and dynamic light scattering measurement. J Colloid Interface Sci 2013;392:27–33.
Miller RJ, Bennett S, Keller AA, Pease S, Lenihan HS. TiO2 nanoparticles are phototoxic to marine phytoplankton. Plos One 2012;7:e30321.
Ottofuelling S, Von der Kammer F, Hofmann T. Commercial titanium dioxide nanoparticles in both natural and synthetic water: comprehensive multidimensional testing and prediction of aggregation behavior. Environ Sci Technol 2011;45:10045–52.
Overbeek JTG, Kruyt HColloid science, vol. I. Amsterdam: Elsevier; 1952. p. 278–86.
Pakarinen K, Petersen EJ, Alvila L, Waissi-Leinonen GC, Akkanen J, Leppanen MT, et al. A screening study on the fate of fullerenes (nC_{60}) and their toxic implications in natural freshwaters. Environ Toxicol Chem 2013;32:1224–32.
Persson P, Lunell S. Binding of bi-isonicotinic acid to anatase TiO2 (101). Sol Energy Mater Sol Cells 2000;63:139–48.
Piccolo A. The supramolecular structure of humic substances. Soil Sci 2001;166:810–32.
Qi J, Ye YY, Wu JJ, Wang HT, Li FT. Dispersion and stability of titanium dioxide nanoparticles in aqueous suspension: effects of ultrasonication and concentration. Water Sci Technol 2013;67:147–51.
Roddick-Lanzilotta AD, McQuillan AJ. An in situ infrared spectroscopic study of glutamic acid and of aspartic acid adsorbed on TiO2: implications for the biocompatibility of titanium. J Colloid Interface Sci 2000;227:48–54.
Song U, Shin M, Lee G, Roh J, Kim Y, Lee EJ. Functional analysis of TiO2 nanoparticle toxicity in three plant species. Biol Trace Elem Res 2013;155:93–103.
Tan XL, Fang M, Li JX, Lu Y, Wang XK. Adsorption of Eu(III) onto TiO2: effect of pH, concentration, ionic strength and soil fulvic acid. J Hazard Mater 2009;168:458–65.
Theron J, Walker JA, Cloete TE. Nanotechnology and water treatment: applications and emerging opportunities. Crit Rev Microbiol 2008;34:43–69.
Thio BJR, Zhou DX, Keller AA. Influence of natural organic matter on the aggregation and deposition of titanium dioxide nanoparticles. J Hazard Mater 2011;189:556–63.
Trouiller B, Reliene R, Westbrook A, Solaimani P, Schiestl RH. Titanium dioxide nanoparticles induce DNA damage and genetic instability in vivo in mice. Cancer Res 2009;69:8784–9.
Verwey E, Overbeek JTG. Theory of the stability of lyophobic colloids, 1948. Amsterdam: Elsevier; 2001.
Wang HT, Keller AA, Clark KK. Natural organic matter removal by adsorption onto magnetic permanently confined micelle arrays. J Hazard Mater 2011;194:156–61.
Wang HT, Keller AA, Li FT. Natural organic matter removal by adsorption onto carbonaceous nanoparticles and coagulation. J Environ Eng Asce 2010;136:1075–81.
Wang HT, Ye YY, Qi J, Li FT, Tang YL. Removal of titanium dioxide nanoparticles by coagulation: effects of coagulants, typical ions, alkalinity and natural organic matters. Water Sci Technol 2013;68:1137–43.
Wiesner MR, Lowry GV, Alvarez P, Dionysiou D, Biswas P. Assessing the risks of manufactured nanomaterials. Environ Sci Technol 2006;40:4336–45.
Wirth SM, Lowry GV, Tilton RD. Natural organic matter alters biofilm tolerance to silver nanoparticles and dissolved silver. Environ Sci Technol 2012;46:12687–96.
Yang K, Lin DH, Xing BS. Interactions of humic acid with nanosized inorganic oxides. Langmuir 2009;25:3571–6.
Yang SP, Bar-Ilan O, Peterson RE, Heideman W, Hamers RJ, Pedersen JA. Influence of humic acid on titanium dioxide nanoparticle toxicity to developing zebrafish. Environ Sci Technol 2013;47:4718–25.
Zhang W, Crittenden J, Li KG, Chen YS. Attachment efficiency of nanoparticle aggregation in aqueous dispersions: modeling and experimental validation. Environ Sci Technol 2012;46:7054–62.
Zhang W, Rattanaudompol US, Li H, Bouchard D. Effects of humic and fulvic acids on aggregation of aqu/nC(60) nanoparticles. Water Res 2013;47:1793–802.
Zhang Y, Chen YS, Westerhoff P, Crittenden J. Impact of natural organic matter and divalent cations on the stability of aqueous nanoparticles. Water Res 2009;43:4249–57.
Zhang Y, Chen YS, Westerhoff P, Hristovski K, Crittenden JC. Stability of commercial metal oxide nanoparticles in water. Water Res 2008;42:2204–12.
Zheng Z, He PJ, Zhang H, Shao LM. Role of dissolved humic substances surrogates on phthalate esters migration from sewage sludge. Water Sci Technol 2008;57:607–12.
Zhou DX, Abdel-Fattah AI, Keller AA. Clay particles destabilize engineered nanoparticles in aqueous environments. Environ Sci Technol 2012;46:7520–6.